Nephrol Dial Transplant (2010) 25: 2134–2141
doi: 10.1093/ndt/gfq063
Advance Access publication 15 February 2010

# Effects of an oral adsorbent on oxidative stress and fibronectin expression in experimental diabetic nephropathy

Sun Ha Lee[1,*], Bo Young Nam[1,*], Ea Wha Kang[2,*], Seung Hyeok Han[2], Jin Ji Li[1,3], Do Hee Kim[1], Seung Hye Kim[1], Seung-Jae Kwak[1], Jung Tak Park[1], Tae Ik Chang[1], Tae-Hyun Yoo[1], Dae Suk Han[1] and Shin-Wook Kang[1]

[1]Yonsei University College of Medicine, Department of Internal Medicine, 134 Shinchon-Dong, Seodaemoon-Gu, Seoul, South Korea, [2]Division of Nephrology, Department of Internal Medicine, NHIC Ilsan Hospital, Goyang, Gyeonggi-do, South Korea and [3]Nephrology and Dialysis Unit, Department of Internal Medicine, The Affiliated Hospital, YanBian University Medical College, JiLin, China

*Correspondence and offprint requests to*: Shin-Wook Kang; E-mail: kswkidney@yumc.yonsei.ac.kr
[*]These authors contributed equally to this work.

## Abstract

**Background.** Previous studies have demonstrated that AST-120 (Kremezin®), a well-known oral adsorbent, inhibits the progression of diabetic (DM) and non-DM chronic kidney disease along with a decrease in oxidative stress. This study was undertaken to investigate whether AST-120 could reduce oxidative stress and ameliorate the development of nephropathy in experimental DM rats with normal renal function.

**Methods.** Rats were injected with diluent (C, $n = 16$) or 65 mg/kg streptozotocin intraperitoneally (DM, $n = 16$), and eight rats from each group were treated with chow containing 5% AST-120. After 3 months, plasma advanced oxidation protein products (AOPP) and total malondialdehyde (MDA) levels, 24-h urinary albumin excretion, and urinary 8-hydroxy-2′-deoxyguanosine (8-OHdG) excretion were determined by ELISA. Glomerular endothelial nitric oxide synthase (eNOS), subunits of nicotinamide adenine dinucleotide phosphate (NADPH) oxidase (gp91phox, p47phox and p22phox), and fibronectin (FN) mRNA and protein expressions were determined by real-time PCR and western blot, respectively. In addition, dichlorodihydrofluorescein diacetate (DCF-DA) staining was performed to detect glomerular reactive oxygen species (ROS) production.

**Results.** Compared to the C group, 24-h urinary albumin excretion was significantly higher in the DM group ($P < 0.01$), and AST-120 treatment significantly reduced albuminuria in DM rats ($P < 0.05$). Glomerular eNOS, gp91phox, p47phox and FN expression were significantly increased in DM rats compared to C rats, and these increases in DM glomeruli were significantly abrogated by AST-120 treatment ($P < 0.05$). The increases in plasma AOPP and MDA levels as well as renal oxidative stress in DM rats, assessed by DCF-DA staining and urinary 8-OHdG excretion rates, were also significantly attenuated by AST-120 treatment ($P < 0.05$).

**Conclusion.** In conclusion, the renoprotective effects of AST-120 in DM nephropathy seem to be associated with the amelioration of enhanced oxidative stress and FN expression under diabetic conditions.

**Keywords:** AST-120; diabetic nephropathy; fibronectin; oxidative stress

## Introduction

Numerous experimental and clinical studies have shown that oxidative stress plays an important role in the development and progression of diabetic nephropathy [1]. High glucose *per se*, transforming growth factor (TGF)-β1 and angiotensin II (AII) are all reported to increase reactive oxygen species (ROS) in cultured mesangial cells, which in turn activates protein kinase C (PKC) and nuclear factor (NF)-κB [2–4]. In addition, pathologic changes in glomeruli and an increase in urinary albumin excretion in diabetic rats were ameliorated by dietary antioxidant supplementation with vitamin E, taurine or lipoic acid, supporting the role of oxidative stress in the pathogenesis of diabetic nephropathy [5–7].

The degree of oxidative stress is determined by the balance between the production of ROS and the antioxidant defence system [8]. In experimental and human diabetes, ROS generation is known to be increased via multiple pathways, including glucose auto-oxidation, increased mitochondrial superoxide production, PKC-dependent activation of nicotinamide adenine dinucleotide phosphate (NADPH) oxidase, uncoupled endothelial nitric oxide synthase (eNOS) activity, formation of advanced glycation end products (AGEs) and stimulation of cellular ROS production by extracellular AGEs through their receptors [1,9]. Among these, the activation of NADPH oxidase

and uncoupling of eNOS mainly contribute to the increase in glomerular superoxide production in experimental diabetic rats [10].

AST-120 (Kremezin®, Kureha-Chemical Co., Tokyo, Japan) is a well-known oral adsorbent which binds and prevents absorption of several biologically active substances such as indole from the gastrointestinal tract [11]. Indole is a precursor of indoxyl sulphate, a well-known uraemic substance, and serum indoxyl sulphate concentrations are increased in patients with decreased renal function [12]. In animal and human studies of renal failure, a close relationship between indoxyl sulphate and oxidative stress has been found [13,14]. Moreover, previous studies have shown that AST-120 treatment inhibits the progression of diabetic [15,16] and non-diabetic chronic kidney disease [17,18] along with decreased oxidative stress [13,19,20]. On the other hand, AST-120 is known to adsorb AGEs such as (carboxymethyl)lysine (CML) [21], which are not only important mediators in the pathogenesis of diabetic nephropathy but also associated with oxidative stress, both *in vivo* and *in vitro* [22,23], suggesting that AST-120 may exert a beneficial effect on diabetic nephropathy.

To date, however, the effect of AST-120 on non-uraemic diabetic kidney disease has never been explored. The present study was undertaken to investigate whether the administration of an oral adsorbent, AST-120, could reduce oxidative stress and ameliorate the development of nephropathy in experimental diabetic rats with normal renal function in terms of extracellular matrix (ECM) accumulation.

## Materials and methods

### *Animals*

All animal studies were conducted under an approved protocol. Thirty-two male Sprague–Dawley rats, weighing 250–280 g, were studied. Half were injected with diluent (control, C) and half with 65 mg/kg streptozotocin (diabetes, DM) intraperitoneally. Blood glucose levels were measured 3 days after streptozotocin injection to confirm the development of diabetes. Control and diabetic rats were then randomly assigned to two groups. One group, composed of eight control and eight diabetic rats, was fed with standard laboratory chow containing 5% AST-120 (Kremezin®), and the other group (8 control and 8 diabetic rats) with standard laboratory chow. All rats were housed in a temperature-controlled room and were given free access to water and chow during the 3-month study period.

Body weights were checked monthly, and kidney weights were measured at the time of sacrifice. Serum glucose was measured monthly, and blood urea nitrogen, creatinine and 24-h urinary albumin were determined by ELISA (Nephrat II, Exocell, Inc., Philadelphia, PA, USA) at the time of sacrifice.

### *Isolation of glomeruli*

Glomeruli were isolated by sieving. Purity of the glomerular preparation was >98% as determined by light microscopy.

### *Isolation of total RNA*

Total glomerular RNA was extracted as described previously [24]. Briefly, 100 µl of RNA STAT-60 reagent (Tel-Test, Inc., Friendswood, TX, USA) was added to the glomeruli, followed by lysis by freezing and thawing three times. Another 700 µl of RNA STAT-60 reagent was added, the mixture was vortexed and stored for 5 min at room temperature, 160 µl of chloroform was added and the mixture was shaken vigorously for 30 s. After 3 min, the mixture was centrifuged at 12 000 *g* for 15 min at 4°C, and the upper aqueous phase containing the extracted RNA was transferred to a new tube. RNA was precipitated from the aqueous phase with 400 µl isopropanol and pelleted by centrifugation at 12 000 *g* for 30 min at 4°C. The RNA precipitate was washed with 70% ice-cold ethanol, dried using a Speed Vac and dissolved in diethyl pyrocarbonate (DEPC)-treated distilled water. Glomerular RNA yield and quality were assessed based on spectrophotometric measurement at wavelengths of 260 and 280 nm.

### *Reverse transcription*

First strand cDNA was made using a Boehringer Mannheim cDNA synthesis kit (Boehringer Mannheim GmbH, Mannheim, Germany). Two microgram of total RNA extracted from sieved glomeruli was reverse transcribed using 10 µM random hexanucleotide primer, 1 mM dNTP, 8 mM $MgCl_2$, 30 mM KCl, 50 mM Tris–HCl, pH8.5, 0.2 mM dithiothreitol, 25 U RNAse inhibitor and 40 U avian myeloblastosis virus (AMV) reverse transcriptase. The mixture was incubated at 30°C for 10 min and 42°C for 1 h, followed by enzyme inactivation at 99°C for 5 min.

### *Real-time PCR*

Using the ABI PRISM® 7700 Sequence Detection System (Applied Biosystems, Foster City, CA, USA), PCR was performed in a total volume of 20 µl per well, containing 10 µl SYBR Green® PCR Master Mix (Applied Biosystems), 5 µl cDNA and 5 pmol sense and antisense primers for eNOS, NADPH oxidase (gp91phox, p47phox and p22phox), fibronectin and 18S. Primer sequences are shown in Table 1. Each sample was run in triplicate in separate tubes to permit quantification of the gene normalized to 18S.

After real-time PCR, the temperature was increased from 60°C to 95°C to construct a melting curve. A control without cDNA was run in parallel with each assay. The cDNA content of each specimen was determined using a comparative threshold cycle ($C_t$) method with $2^{-\Delta\Delta Ct}$. The results were given as relative expression of a specific gene normalized to the 18S housekeeping gene. Signals from control glomeruli were considered a relative value of 1.0.

### *Western blot analysis*

Sieved glomeruli were lysed in sodium dodecyl sulphate (SDS) sample buffer [2% sodium dodecyl sulphate, 10 mM Tris–HCl, pH6.8, 10% (vol/vol) glycerol]. Aliquots of 50-µg protein were treated with Laemmli sample buffer, were heated at 100°C for 5 min and were electrophoresed at 50µg per lane in a 8–12% acrylamide denaturing SDS–polyacrylamide gel. To detect dimeric form of eNOS, aliquots of 50-µg protein samples were treated with Laemmli sample buffer without mercaptoethanol, were not heated and were electrophoresed in the cold room (low-temperature SDS–PAGE). The proteins were then transferred to a Hybond enhanced chemiluminescence (ECL) membrane using a Hoeffer semi-dry blotting apparatus (Hoeffer Instruments, San Francisco, CA, USA). The membrane was incubated in blocking buffer A (1× PBS, 0.1% Tween-20 and 8% nonfat milk) for 1h at room temperature and incubated overnight at 4°C in a 1:500 dilution of polyclonal antibody detecting eNOS, gp91phox, p47phox, p22phox, 4-hydroxy-2-nonenal (4-HNE) (Santa Cruz Biotechnology, Inc., Santa Cruz, CA, USA), fibronectin (Chemicon International, Inc., Temecula, CA, USA) or β-actin (Santa Cruz Biotechnology, Inc.). The membrane was then washed once for 15 min and twice for 5 min in 1× PBS with 0.1% Tween-20 and incubated in buffer A with horseradish peroxidase-linked goat anti-mouse or anti-rabbit immunoglobulin G (IgG) (Amersham Life Science, Inc., Arlington Heights, IL, USA) at 1:1000 dilution. The washes were repeated, and the membrane was developed with chemiluminescent reagents (ECL; Amersham Life Science, Inc.). Band densities were measured using TINA image software (Raytest, Straubenhardt, Germany).

### *Dichlordihydrofluorescin diacetate (DCF-DA) staining*

The fluorescent dye, 2′,7′-DCF-DA (Invitrogen, Carlsbad, CA, USA), was used to detect the presence of ROS in sieved glomeruli. 2′,7′-DCF-DA diffuses across cell membranes and is hydrolysed by non-specific cellular esterases to the non-fluorescent compound dichlorofluorescein (DCFH), which is trapped predominantly within the cell. In the presence of ROS, DCFH rapidly undergoes one-electron oxidation to the highly fluorescent

**Table 1.** Sequences of primers used in this study

| Name | Forward | Reverse | bp |
|---|---|---|---|
| eNOS | GGCTGCTGCCCGAGATATC | GGCAGTAATTGCAGGCTCTCA | 93 |
| gp91phox | CCTGCAGCCTGCCTGAA | AAGGAGAGGAGATTCCGACACA | 63 |
| p47phox | CCGGTGAGATCCACACAGAA | TGCACGCTGCCCATCAT | 207 |
| p22phox | GGTGAGCAGTGGACTCCCATT | TGGTAGGTGGCTGCTTGATG | 79 |
| Fibronectin | TGACAACTGCCGTAGACCTGG | TACTGGTTGTAGGTGTGGCCG | 72 |
| 18S | AGTCCCTGCCCTTTGTACACA | GATCCGAGGGCCTCACTAAAC | 67 |

compound dichlorofluorescein (DCF). Sieved glomeruli were plated into two-well Lab-Tek®II Chamber Slides (Nalge Nunc International Corp., Naperville, IL, USA) and rinsed with PBS, and the PBS was replaced with Dulbecco's Modified Eagle's Medium (DMEM) without phenol red. $H_2$-DCF-DA was dissolved in DMSO to a final 50-mM stock solution, which was further diluted in DMEM to a final concentration of 50 μM. Glomeruli were then incubated at 37°C for 5 min and subsequently rinsed two additional times with DMEM and imaged immediately. Exposure time was kept at <1 s to avoid photo-oxidation of the ROS-sensitive dyes and was kept constant for all treatments. At least three independent fields were chosen for each condition, and 5–10 glomeruli in a given field were used to quantify the fluorescence signal. Formation of DCF was monitored in a fluorescent microplate reader with emission at 520 nm and excitation at 500 nm. Results were expressed as fold of control.

*Measurement of plasma advanced oxidation protein products (AOPP) and total malondialdehyde (MDA) levels*

Plasma levels of AOPP were determined based on a spectrophotometric measurement as previously described by Witko-Sarsat *et al*. [25], and plasma total MDA concentrations by commercially available kit (Oxis International, Inc., Foster City, CA, USA) according to manufacturer's instructions. For AOPP measurement, 200 μl of plasma diluted 1:5 with PBS, 200 μl of chloramines-T (0–100 μmol/l) for calibration and 200 μl of PBS as blank were applied on a 96-well microtitre plate. Then, 10 μl of 1.16 M potassium iodide and 20 μl of acetic acid were added, and the absorbance of the reaction mixture was immediately read using a microplate reader at a wavelength of 340 nm. For total MDA, 210 μl of plasma or serial dilution of tetraethoxypropane as standard, 11 μl of butylated hydroxytoluene and 5.3 μl of concentrated HCl were applied on microfuge tubes and were incubated at 60°C for 80 min. After cooling to room temperature, 680 μl of diluted R1 (*N*-methyl-2-phenylindole in acetonitrile) was added, and the mixtures were centrifuged at 13 000 *g* for 5 min. After centrifugation, the supernatants were transferred to new tubes. Then, 115 μl of HCl was added, incubated at 45°C for 60 min and centrifuged at 13 000 *g* for 5 min. Total MDA levels in the supernatant were determined based on spectrophotometric measurement at a wavelength of 586 nm.

*Measurement of urine 8-hydroxydeoxyguanosine (8-OHdG) levels*

Urine specimens were centrifuged at 1500 rpm for 10 min to remove particulates (Eppendorf Centrifuge 5415R, Hamburg, Germany). The supernatants were used, and 8-OHdG levels were measured by using a competitive *in vitro* enzyme-linked immunosorbent assay (ELISA) kit (Bioxytech, OXIS Health Products, Inc., Portland, OR, USA). A 50-μl urine sample and 50 μl of reconstituted primary antibody were added to each well of 8-OHdG-coated microtitre plates and incubated at 37°C for 1 h. Plates were washed three times with phosphate-buffered saline, and horseradish peroxidase-conjugated secondary antibody was added. After incubation at 37°C for 1 h, unbound secondary antibody was removed, and the plate was washed again three times. The amount of antibody bound to the plate was determined by the development of colour intensity after the addition of a substrate containing 3,3′,5,5′-tetra-methyl-benzidine. The reaction was terminated by the addition of phosphoric acid, and the absorbance was measured using a computer-controlled spectrophotometric plate reader at a wavelength of 450 nm. The concentration of 8-OHdG was interpolated from a standard curve drawn with the assistance of logarithmic transformation. The detection range of the ELISA assay was 0.5–200 ng/ml.

*Measurement of serum indoxyl sulphate and AGE concentrations*

Serum indoxyl sulphate concentrations were measured by high-performance liquid chromatography (HPLC). Serum samples (10 μl) were analysed for 10 min with a mobile phase, 5% tetrahydrofuran/0.1 M $KH_2PO_4$ (pH 6.5), at a flow rate of 1 ml/min and with fluorescence detection with excitation at 295 nm and emission at 390 nm.

The concentrations of AGEs in serum were determined using a commercial ELISA kit (Uscnlife Sciences & Technology Co., Ltd, Wuhan, China) according to the manufacturer's protocol. Briefly, 100 μl of standard solution or sample was added into a 96-well microplate coated with anti-rat AGEs antibody and incubated at 37°C for 2 h. After removal of solution, 100 μl of detection reagent A solution was added to each well and incubated at 37°C for 1 h. Plates were washed three times with wash buffer, and 100 μl of detection reagent B solution was added. After another 1-h incubation at 37°C and four washes, addition of 90 μl of substrate solution was followed by a 30-min incubation at 37°C and in the dark. Finally, 50 μl of stop solution was added, and the optical density was determined at 450 nm using an ELISA microtitre plate reader. The kit for rat AGEs was species-specific, and the minimum detectable concentration was typically <1.95 ng/ml.

*Statistical analysis*

All values are expressed as the mean ± standard error of the mean (SEM). Statistical analyses were performed using the statistical package SPSS for Windows version 11.0 (SPSS, Inc., Chicago, IL, USA). Results were analysed using the Kruskal–Wallis non-parametric test for multiple comparisons. Significant differences by the Kruskal–Wallis test were confirmed by the Mann–Whitney *U*-test. *P*-values <0.05 were considered statistically significant.

## Results

### *Animal data*

All animals gained weight over the 3-month experimental period, but weight gain was highest in C rats ($P < 0.01$). The ratios of kidney weight to body weight were significantly higher in DM (1.34 ± 0.09%) and DM + AST-120 rats (1.28 ± 0.10%) than in C (0.62 ± 0.04%) and C + AST-120 rats (0.64 ± 0.06%) ($P < 0.01$). The mean blood glucose levels of C, C + AST-120, DM and DM + AST-120 rats were 106.4 ± 5.7, 110.5 ± 4.2, 495.0 ± 8.9 and 482.6 ± 6.3 mg/dl, respectively ($P < 0.01$). The mean creatinine clearance was higher in DM (6.18 ± 0.97 ml/min/kg body weight) and DM + AST-120 rats (5.98 ± 0.74 ml/min/kg body weight) relative to C rats (4.23 ± 0.58 ml/min/kg body weight) but did not reach statistical significance. Compared to the C group (0.40 ± 0.06 mg/day), 24-h urinary albumin excretion was significantly higher in the DM group (1.99 ± 0.17 mg/day, $P < 0.01$), and AST-120 treatment significantly reduced albuminuria in DM rats (1.04 ± 0.19 mg/day, $P < 0.05$) (Table 2).

**Table 2.** Animal data

| | C | C + AST | DM | DM + AST |
|---|---|---|---|---|
| Body weight (g) | 557.8 ± 18.8 | 545.0 ± 15.1 | 292.1 ± 9.6* | 281.3 ± 9.5* |
| Kwt/Bwt ($\times 10^{-2}$) | 0.62 ± 0.04 | 0.64 ± 0.06 | 1.34 ± 0.09* | 1.28 ± 0.10* |
| Glucose (mg/dl) | 106.4 ± 5.7 | 110.5 ± 4.2 | 495.0 ± 8.9* | 482.6 ± 6.3* |
| CCr (ml/min/kg Bwt) | 4.23 ± 0.58 | 4.47 ± 0.67 | 6.18 ± 0.97 | 5.98 ± 0.74 |
| UAE (mg/day) | 0.40 ± 0.06 | 0.36 ± 0.08 | 1.99 ± 0.17* | 1.04 ± 0.19** |

Values are means ± SE.Kwt, kidney weight; Bwt, body weight; CCr, creatinine clearance; UAE, urinary albumin excretion.*$P < 0.01$ *vs*. C and C + AST, **$P < 0.05$ *vs*. DM.

### *Effects of AST-120 on glomerular eNOS, subunits of NADPH oxidase and fibronectin mRNA expression*

Compared to C rats, glomerular eNOS, gp91phox and p47phox mRNA expression were significantly increased in DM rats by 2.1-, 3.3- and 2.7-fold, respectively ($P < 0.05$), and these increases were significantly abrogated by AST-120 treatment ($P < 0.05$). In contrast, there was no difference in glomerular p22phox mRNA expression among the four groups (Figure 1). Fibronectin mRNA expression was also increased in DM compared to C glomeruli, and AST-120 treatment significantly ameliorated this increase ($P < 0.05$) (Figure 1).

### *Effects of AST-120 on glomerular eNOS, subunits of NADPH oxidase and fibronectin protein expression*

Similar to the mRNA results, glomerular eNOS, gp91phox and p47phox protein expression assessed by western blot were significantly increased in DM compared to C rats, and these increases were significantly attenuated by AST-120 treatment ($P < 0.05$). In contrast, there was no difference in glomerular p22phox protein expression among the four groups. Fibronectin protein expression was also significantly increased in DM glomeruli, and AST treatment significantly inhibited this increase ($P < 0.05$) (Figure 2). To elucidate whether the increase in eNOS protein expression in DM glomeruli was due to increased eNOS uncoupling, Western blot with low-temperature SDS-PAGE was performed and revealed that uncoupled eNOS protein expression was increased in DM glomeruli, which was abrogated by the administration of AST-120 (Figure 3).

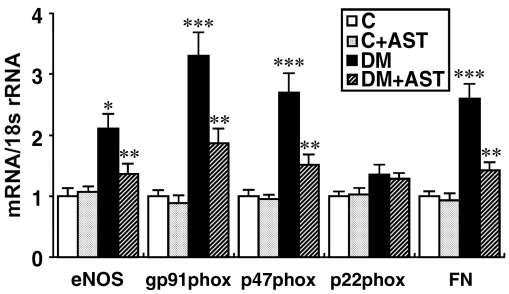


**Fig. 1.** Glomerular eNOS, subunits of NADPH oxidase and fibronectin mRNA expression assessed by real-time PCR in C, C + AST-120 (AST), DM and DM + AST groups. Compared to C rats, glomerular eNOS, gp91phox, p47phox and fibronectin (FN) mRNA/18S rRNA ratios were significantly increased in DM rats by 2.1-, 3.3-, 2.7- and 2.6-fold, respectively, and these increases were significantly abrogated by AST-120 treatment. In contrast, there was no difference in glomerular p22phox mRNA expression among the four groups. *$P < 0.05$ *vs*. C and C + AST, **$P < 0.05$ *vs*. DM, ***$P < 0.01$ *vs*. C and C + AST.

### *Effect of AST-120 on glomerular ROS production*

Glomerular ROS production was evaluated by determining the fluorescent intensity of DCF. DCF fluorescence intensity was 2.6-fold higher in DM compared to C glomeruli ($P < 0.05$), and this increase was significantly ameliorated by AST-120 treatment ($P < 0.05$) (Figure 4).

### *Effects of AST-120 on glomerular 4-HNE protein expression*

The expression of 4-HNE protein complex, which reflexes ROS-mediated lipid peroxidation [26], was increased in

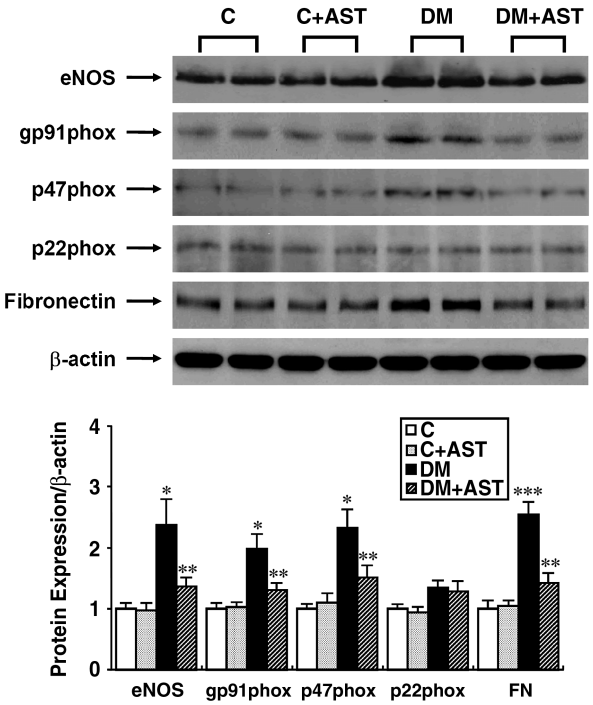


**Fig. 2.** A representative western blot of glomerular eNOS, gp91phox, p47phox, p22phox, fibronectin (FN) and β-actin in C, C + AST-120 (AST), DM and DM + AST groups (representative of four blots). Compared to C rats, glomerular eNOS, gp91phox, p47phox and fibronectin protein expression were significantly increased in DM rats by 2.4-, 2.0-, 2.3- and 2.5-fold, respectively, and these increases were significantly ameliorated by the administration of AST-120. In contrast, there was no difference in glomerular p22phox protein expression among the four groups. *$P < 0.05$ *vs*. C and C + AST, **$P < 0.05$ *vs*. DM, ***$P < 0.01$ *vs*. C and C + AST.

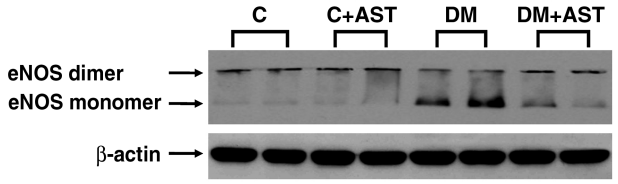


**Fig. 3.** A representative western blot of eNOS with C, C + AST-120 (AST), DM and DM + AST glomeruli after low temperature SDS–PAGE electrophoresis (representative of four blots). The expression of uncoupled eNOS protein was increased in DM relative to C glomeruli, and AST-120 treatment in DM rats attenuated this increase.

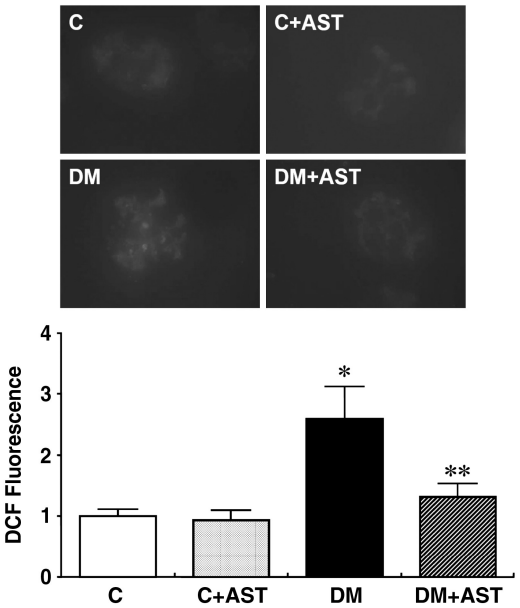


**Fig. 4.** A representative DCF-DA staining for glomerular ROS production in C, C + AST-120 (AST), DM and DM + AST groups. The intensity of DCF fluorescence was 2.6-fold higher in DM compared to C glomeruli, and this increase was significantly inhibited by AST-120 treatment. *$P < 0.05$ *vs*. C and C + AST, **$P < 0.05$ *vs*. DM.

DM relative to C glomeruli, and AST-120 treatment attenuated this increase in glomerular 4-HNE protein expression in DM rats (Figure 5).

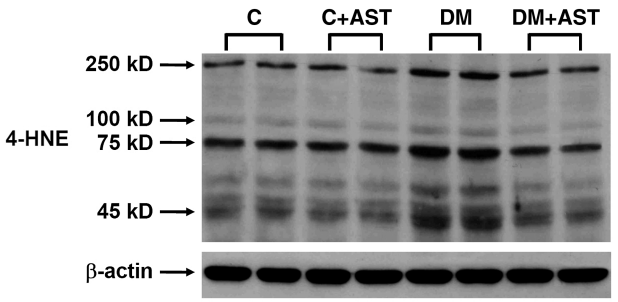


**Fig. 5.** A representative western blot of glomerular 4-HNE protein complex in C, C + AST-120 (AST), DM and DM + AST groups (representative of four blots). The expression of 4-HNE protein was increased in DM relative to C glomeruli, and AST-120 treatment abrogated this increase in glomerular 4-HNE protein expression in DM rats.

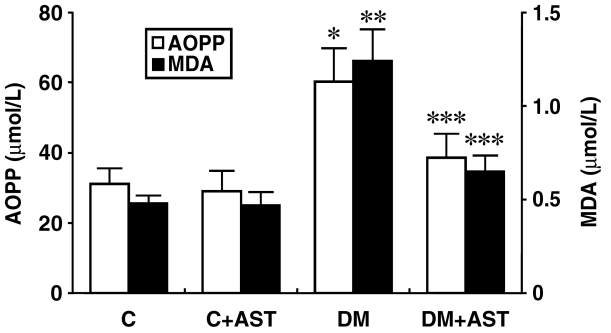


**Fig. 6.** Plasma concentrations of AOPP and total MDA assessed by ELISA in C, C + AST-120 (AST), DM and DM + AST groups. Plasma AOPP and MDA levels were significantly higher in DM compared to C rats, and these increases were significantly ameliorated by the administration of AST-120. *$P < 0.05$ *vs*. C and C + AST, **$P < 0.01$ *vs*. C and C + AST, ***$P < 0.05$ *vs*. DM.

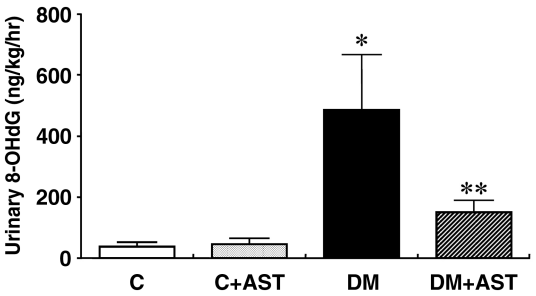


**Fig. 7.** Urinary 8-OHdG excretion rates assessed by ELISA in C, C + AST-120 (AST), DM and DM + AST groups. Urinary 8-OHdG excretion rates were significantly higher in DM compared to C rats, and this increase was significantly attenuated by AST-120 treatment. *$P < 0.001$ *vs*. C and C + AST, **$P < 0.01$ *vs*. DM.

### *Effect of AST-120 on plasma AOPP and total MDA levels*

Plasma concentrations of AOPP and total MDA, which represent ROS-mediated protein [25] and lipid peroxidation [26], respectively, were significantly increased in DM (AOPP, 60.6 ± 9.6 μmol/l; MDA, 1.24 ± 0.17 μmol/l) compared to C rats (AOPP, 31.3 ± 4.5 μmol/l, $P < 0.05$; MDA, 0.48 ± 0.07 μmol/l, $P < 0.01$), and these increases were significantly inhibited by the administration of AST-120 (AOPP, 38.9 ± 6.9 μmol/l; MDA, 0.65 ± 0.08 μmol/l) ($P < 0.05$) (Figure 6).

### *Effect of AST-120 on urinary 8-OHdG excretion*

Urinary 8-OHdG excretion rates were significantly higher in DM than C rats (486.9 ± 182.3 *vs*. 37.3 ± 13.8 ng/kg/h, $P < 0.001$), and this increase was significantly abrogated by AST-120 treatment (151.2 ± 38.4 ng/kg/h) ($P < 0.01$) (Figure 7).

### *Effect of AST-120 on serum indoxyl sulphate and AGEs concentrations*

The mean serum indoxyl sulphate levels of C, C + AST-120, DM and DM + AST-120 rats were 0.10 ± 0.02, 0.09 ± 0.01, 0.11 ± 0.02 and 0.08 ± 0.01 mg/dl, respectively, which were comparable among the four groups. In con-

trast, serum AGEs concentrations were significantly higher in DM (11.8 ± 2.1 ng/ml) compared to C rats (5.8 ± 0.7 ng/ml) and C + AST-120 rats (5.3 ± 0.8 ng/ml) ($P < 0.05$), and AST-120 treatment significantly ameliorated this increase (7.0 ± 1.2 ng/ml) ($P < 0.05$).

## Discussion

Recent experimental and clinical studies have demonstrated that AST-120, an oral absorbent, inhibits the progression of diabetic [15,16] and non-diabetic chronic kidney disease [17,18] along with a decrease in oxidative stress [13,19,20], but the effect of AST-120 on non-uraemic kidney disease has never been explored. This study demonstrates for the first time that AST-120 treatment inhibits the increase in albuminuria and enhanced glomerular fibronectin expression in diabetic rats. In addition, the results of this study suggest that reduced oxidative stress may contribute to these effects of AST-120.

Oxidative stress involves various molecules collectively called ROS, which include superoxide anions, hydrogen peroxide, NO, and peroxynitrite and play a pivotal role in the pathogenesis of diabetic nephropathy [1]. High glucose increased production of DCF-sensitive ROS in cultured mesangial cells in a time-dependent manner [2], and this increase in ROS is known to be dependent on PKC, NADPH oxidase and the mitochondrial electron gradient [1–3]. TGF-β1 and AII also increased ROS production in cultured mesangial cells in a NADPH oxidase-dependent manner [3,4]. In addition, ROS are known to mediate both *in vivo* and *in vitro* activation of PKC, NF-κB, TGF-β1, fibronectin and plasminogen activator inhibitor (PAI)-1 under diabetic conditions [2,3,27]. In diabetic animals, increased activities of glomerular PKC-δ and PKC- were also inhibited by treatment with taurine, an antioxidant [28]. Similarly, the antioxidant treatment suppressed the increase in glomerular TGF-β1 and fibronectin mRNA expression, and ameliorated glomerular thickening, mesangial expansion and proteinuria in diabetic rats [29,30]. The results of our study show that fibronectin expression is increased in diabetic glomeruli, and this increase in fibronectin expression is attenuated by AST-120 treatment, along with reduced plasma AOPP and MDA levels, glomerular ROS production and 4-HNE expression, and urinary 8-OHdG excretion. This suggests that this change in fibronectin expression is in part mediated by alleviation of enhanced oxidative stress by AST-120 in diabetic rats.

NADPH oxidase is a major source of oxidants in renal cells such as tubular epithelial cells and glomerular mesangial cells [31]. NADPH oxidase was originally found in neutrophils, and it is composed of five subunits: two membrane-associated subunits (gp91phox and p22phox) and three major cytosolic subunits (p67phox, p47phox and p40phox) [31]. Under diabetic conditions, the expression of some subunits of NADPH oxidase is known to be increased *in vitro* and *in vivo*, resulting in enhanced oxidative stress levels [32,33]. Similar to the previous reports, the present study shows that gp91phox and p47phox mRNA and protein expression are increased in diabetic glomeruli, and these increases are ameliorated by AST-120 treatment, suggesting that AST-120 may reduce oxidative damage in the diabetic kidney via the inhibition of NADPH oxidase-mediated ROS production. Among the subunits of NADPH oxidase, there was no difference in p22phox expression among the study groups. Even though Kitada *et al*. [33] also found no difference in p22phox expression between control and diabetic glomeruli, the reasons for the divergence of changes in NAPDH oxidase subunits are not clear and need to be investigated further.

In addition to NADPH oxidase, increased ROS generation under diabetic conditions is attributed to changes in NOS, xanthine oxidase, cyclooxygenase and lipoxygenase [8]. Particularly, in diabetic nephropathy, the major sources of ROS are known to be NADPH oxidase and uncoupled NOS, which reduces glomerular NO production despite increased expression of eNOS [10]. In addition, eNOS itself is also found to produce $O2^{-}$, which requires $Ca^{2+}$/calmodulin and is primarily regulated by tetrahydrobiopterin rather than L-arginine [34]. Although there are conflicting results on the expression of eNOS in diabetic nephropathy, many studies have shown that eNOS expression is increased in animal [10,32] and human [35] diabetic glomeruli, which is consistent with the findings of this study. In addition, the results of the present study also show that the increase in eNOS expression is mainly attributed to the increase in uncoupled eNOS.

The results of this study suggest that AST-120 reduces oxidative stress in diabetic glomeruli via the inhibition of NADPH oxidase- and uncoupled eNOS-mediated ROS production, resulting in decreases in albuminuria and glomerular fibronectin expression. However, this leaves us with another question: how does AST-120 abrogate the up-regulation of these genes expression under diabetic conditions? AST-120 is an oral adsorbent that consists of fine spherical carbonic particles of ~0.2–0.4 mm in diameter and can absorb low-molecular-weight substances such as indole [11] which is a precursor of indoxyl sulphate, one of the well-known circulating uraemic toxins. Recently, some studies have suggested a close association between indoxyl sulphate and oxidative stress. AST-120 suppressed the progression of renal failure in 5/6 nephrectomized rats, at least in part by the amelioration of oxidative stress as assessed by urinary excretion of acrolein and 8-OHdG [19]. In addition, Tumur and Niwa [36] and Muteliefu *et al*. [37] found that indoxyl sulphate induced significant production of ROS in cultured human umbilical vein endothelial cells and cultured human aortic smooth muscle cells, respectively, via inducing NADPH oxidase expression. Therefore, we hypothesized that AST-120 may reduce indoxyl sulphate levels in diabetic rats, leading to the attenuation of NADPH oxidase expression and subsequently minimizing oxidative stress. However, there was no difference in serum indoxyl sulphate concentrations among the study groups. It seems that similar levels of serum indoxyl sulphate are probably due to the comparable renal function between control and diabetic rats. On the other hand, AST-120 is also known to adsorb hippuric acid, *p*-cresol and AGEs, including methylglyoxal and CML, all of which are known to be associated with oxidative stress [21,38]. Since AGEs play an important role in the patho-

genesis of diabetic nephropathy and induce ROS generation through stimulation of membrane-bound NADPH oxidase [39], we next considered AGEs as candidate substances responsible for the beneficial effects of AST-120 and found that serum AGEs concentrations were significantly increased in diabetic rats, and this increase was significantly inhibited by AST-120 treatment. These findings suggest that the inhibitory effect of AST-120 on NAPDH oxidase expression seems to be partly mediated by reducing AGEs levels in non-uraemic diabetic rats.

In conclusion, AST-120 treatment alleviates oxidative stress and abrogates the increase in fibronectin expression in diabetic nephropathy. These effects seem to be associated with the amelioration of enhanced NAPDH oxidase and uncoupled eNOS expression under diabetic conditions. These findings provide a new perspective on the renoprotective effects of AST-120 in diabetic nephropathy.

*Acknowledgements.* This work was supported by the Brain Korea 21 (BK21) Project for Medical Sciences, Yonsei University and the Korea Science and Engineering Foundation (KOSEF) grant funded by the Korea government (MOST) (R01-2007-000-20263-0 and R13-2002-054-04001-0).

*Conflict of interest statement*. None declared.

## References

1. Forbes JM, Coughlan MT, Cooper ME. Oxidative stress as a major culprit in kidney disease in diabetes. *Diabetes* 2008; 57: 1446–1454
2. Ha H, Yu MR, Choi YJ *et al*. Role of high glucose-induced nuclear factor-kappaB activation in monocyte chemoattractant protein-1 expression by mesangial cells. *J Am Soc Nephrol* 2002; 13: 894–902
3. Lee HB, Yu MR, Yang Y *et al*. Reactive oxygen species-regulated signaling pathways in diabetic nephropathy. *J Am Soc Nephrol* 2003; 14: S241–S245
4. Jaimes EA, Galceran JM, Raij L. Angiotensin II induces superoxide anion production by mesangial cells. *Kidney Int* 1998; 54: 775–784
5. Trachtman H, Futterweit S, Maesaka J *et al*. Taurine ameliorates chronic streptozocin-induced diabetic nephropathy in rats. *Am J Physiol* 1995; 269: F429–F438
6. Craven PA, DeRubertis FR, Kagan VE *et al*. Effects of supplementation with vitamin C or E on albuminuria, glomerular TGF-beta, and glomerular size in diabetes. *J Am Soc Nephrol* 1997; 8: 1405–1414
7. Melhem MF, Craven PA, Derubertis FR. Effects of dietary supplementation of alpha-lipoic acid on early glomerular injury in diabetes mellitus. *J Am Soc Nephrol* 2001; 12: 124–133
8. Droge W. Free radicals in the physiological control of cell function. *Physiol Rev* 2002; 82: 47–95
9. Brownlee M. Biochemistry and molecular cell biology of diabetic complications. *Nature* 2001; 414: 813–820
10. Satoh M, Fujimoto S, Haruna Y *et al*. NAD(P)H oxidase and uncoupled nitric oxide synthase are major sources of glomerular superoxide in rats with experimental diabetic nephropathy. *Am J Physiol Renal Physiol* 2005; 288: F1144–F1152
11. Niwa T, Miyazaki T, Hashimoto N *et al*. Suppressed serum and urine levels of indoxyl sulfate by oral sorbent in experimental uremic rats. *Am J Nephrol* 1992; 12: 201–206
12. Niwa T, Takeda N, Tatematsu A *et al*. Accumulation of indoxyl sulfate, an inhibitor of drug-binding, in uremic serum as demonstrated by internal-surface reversed-phase liquid chromatography. *Clin Chem* 1988; 34: 2264–2267
13. Taki K, Niwa T. Indoxyl sulfate-lowering capacity of oral sorbents affects the prognosis of kidney function and oxidative stress in chronic kidney disease. *J Ren Nutr* 2007; 17: 48–52
14. Owada S, Goto S, Bannai K *et al*. Indoxyl sulfate reduces superoxide scavenging activity in the kidneys of normal and uremic rats. *Am J Nephrol* 2008; 28: 446–454
15. Sanaka T, Akizawa T, Koide K *et al*. Protective effect of an oral adsorbent on renal function in chronic renal failure: determinants of its efficacy in diabetic nephropathy. *Ther Apher Dial* 2004; 8: 232–240
16. Shimizu H, Okada S, Shinsuke OI *et al*. Kremezin (AST-120) delays the progression of diabetic nephropathy in Japanese type 2 diabetic patients. *Diabetes Care* 2005; 28: 2590
17. Owada A, Nakao M, Koike J *et al*. Effects of oral adsorbent AST-120 on the progression of chronic renal failure: a randomized controlled study. *Kidney Int Suppl* 1997; 63: S188–S190
18. Schulman G, Agarwal R, Acharya M *et al*. A multicenter, randomized, double-blind, placebo-controlled, dose-ranging study of AST-120 (Kremezin) in patients with moderate to severe CKD. *Am J Kidney Dis* 2006; 47: 565–577
19. Nakagawa N, Hasebe N, Sumitomo K *et al*. An oral adsorbent, AST-120, suppresses oxidative stress in uremic rats. *Am J Nephrol* 2006; 26: 455–461
20. Shimoishi K, Anraku M, Kitamura K *et al*. An oral adsorbent, AST-120 protects against the progression of oxidative stress by reducing the accumulation of indoxyl sulfate in the systemic circulation in renal failure. *Pharm Res* 2007; 24: 1283–1289
21. Ueda S, Yamagishi S, Takeuchi M *et al*. Oral adsorbent AST-120 decreases serum levels of AGEs in patients with chronic renal failure. *Mol Med* 2006; 12: 180–184
22. Pugliese G, Pricci F, Romeo G *et al*. Upregulation of mesangial growth factor and extracellular matrix synthesis by advanced glycation end products via a receptor-mediated mechanism. *Diabetes* 1997; 46: 1881–1887
23. Suzuki D, Miyata T, Saotome N *et al*. Immunohistochemical evidence for an increased oxidative stress and carbonyl modification of proteins in diabetic glomerular lesions. *J Am Soc Nephrol* 1999; 10: 822–832
24. Kang SW, Adler SG, Lapage J *et al*. p38 MAPK and MAPK kinase 3/6 mRNA and activities are increased in early diabetic glomeruli. *Kidney Int* 2001; 60: 543–552
25. Witko-Sarsat V, Gausson V, Nguyen AT *et al*. AOPP-induced activation of human neutrophil and monocyte oxidative metabolism: a potential target for *N*-acetylcysteine treatment in dialysis patients. *Kidney Int* 2003; 64: 82–91
26. Esterbauer H, Schaur RJ, Zollner H. Chemistry and biochemistry of 4-hydroxynonenal, malonaldehyde and related aldehydes. *Free Radic Biol Med* 1991; 11: 81–128
27. Lee EA, Seo JY, Jiang Z *et al*. Reactive oxygen species mediate high glucose-induced plasminogen activator inhibitor-1 up-regulation in mesangial cells and in diabetic kidney. *Kidney Int* 2005; 67: 1762–1771
28. Ha H, Yu MR, Choi YJ *et al*. Activation of protein kinase c-delta and c-epsilon by oxidative stress in early diabetic rat kidney. *Am J Kidney Dis* 2001; 38: S204–S207
29. Ha H, Lee SH, Kim KH. Effects of rebamipide in a model of experimental diabetes and on the synthesis of transforming growth factor-beta and fibronectin, and lipid peroxidation induced by high glucose in cultured mesangial cells. *J Pharmacol Exp Ther* 1997; 281: 1457–1462
30. Melhem MF, Craven PA, Liachenko J *et al*. Alpha-lipoic acid attenuates hyperglycemia and prevents glomerular mesangial matrix expansion in diabetes. *J Am Soc Nephrol* 2002; 13: 108–116
31. Geiszt M, Leto TL. The Nox family of NAD(P)H oxidases: host defense and beyond. *J Biol Chem* 2004; 279: 51715–51718
32. Onozato ML, Tojo A, Goto A *et al*. Oxidative stress and nitric oxide synthase in rat diabetic nephropathy: effects of ACEI and ARB. *Kidney Int* 2002; 61: 186–194
33. Kitada M, Koya D, Sugimoto T *et al*. Translocation of glomerular p47phox and p67phox by protein kinase C-beta activation is required for oxidative stress in diabetic nephropathy. *Diabetes* 2003; 52: 2603–2614
34. Xia Y, Tsai AL, Berka V *et al*. Superoxide generation from endothelial nitric-oxide synthase. A Ca2+/calmodulin-dependent and

tetrahydrobiopterin regulatory process. *J Biol Chem* 1998; 273: 25804–25808
35. Hohenstein B, Hugo CP, Hausknecht B *et al*. Analysis of NO-synthase expression and clinical risk factors in human diabetic nephropathy. *Nephrol Dial Transplant* 2008; 23: 1346–1354
36. Tumur Z, Niwa T. Indoxyl sulfate inhibits nitric oxide production and cell viability by inducing oxidative stress in vascular endothelial cells. *Am J Nephrol* 2009; 29: 551–557
37. Muteliefu G, Enomoto A, Jiang P *et al*. Indoxyl sulphate induces oxidative stress and the expression of osteoblast-specific proteins in vascular smooth muscle cells. *Nephrol Dial Transplant* 2009; 24: 2051–2058
38. Niwa T, Ise M, Miyazaki T *et al*. Suppressive effect of an oral sorbent on the accumulation of *p*-cresol in the serum of experimental uremic rats. *Nephron* 1993; 65: 82–87
39. Wautier MP, Chappey O, Corda S *et al*. Activation of NADPH oxidase by AGE links oxidant stress to altered gene expression via RAGE. *Am J Physiol Endocrinol Metab* 2001; 280: E685–E694

*Received for publication: 10.7.09; Accepted in revised form: 25.1.10*

Nephrol Dial Transplant (2010) 25: 2141–2149
doi: 10.1093/ndt/gfp768
Advance Access publication 19 January 2010



# Endothelial pro-atherosclerotic response to extracellular diabetic-like environment: Possible role of thioredoxin-interacting protein

Tali Zitman-Gal[1], Janice Green[1], Metsada Pasmanik-Chor[2], Varda Oron-Karni[2] and Jacques Bernheim[1,3]

[1]Renal Physiology Laboratory, Department of Nephrology and Hypertension, Meir Medical Center, Kfar Saba, Israel, [2]Bioinformatics Unit, The G. S. Wise Faculty of Life Sciences, Tel Aviv University, Tel Aviv, Israel, and [3]Sackler Faculty of Medicine Tel Aviv University, Tel Aviv, Israel

*Correspondence and offprint requests to*: Tali Zitman-Gal; E-mail: tali.gal@clalit.org.il

## Abstract

**Background.** High blood and tissue concentrations of glucose and advanced glycation end-products (AGEs) are thought to play an important role in the development of vascular diabetic complications. Therefore, the impact of extracellular AGEs and different glucose concentrations was evaluated by studying the gene expressions and the underlying cellular pathways involved in the development of inflammatory pro-atherosclerotic processes observed in cultured endothelial cells.

**Methods.** Fresh human umbilical vein cord endothelial cells (HUVEC) were treated in the presence of elevated extracellular glucose concentrations (5.5–28 mmol/l) with and without AGE-human serum albumin (HSA). Affymetrix GeneChip® Human Gene 1.0 ST arrays were used for gene expression analysis (total 20 chips). Genes of interest were further validated using real-time PCR and western blot techniques.

**Results.** Microarray analysis revealed significant changes in some gene expressions in the presence of the different stimuli, suggesting that different pathways are involved. Six genes were selected for validation as follows: thioredoxin-interacting protein (*TXNIP*), thioredoxin (*TXN*), nuclear factor of kappa B (*NF-κB*), interleukin 6 (*IL6*), interleukin 8 (*IL8*) and receptor of advanced glycation end-products (*RAGE*). Interestingly, it was found that the association of AGEs together with the highest pathophysiological concentration of glucose (28 mmol/l) diminished the expression of these specific genes, excluding TXN.

**Conclusions.** In the present model that mimics a diabetic environment, the relatively short-term experimental conditions used showed an unexpected blunting action of AGEs in the presence of the highest glucose concentration (28 mmol/l). The interactive cellular pathways involved in these processes should be further investigated.

**Keywords:** advanced glycation end-products; diabetes; endothelial cells; thioredoxin-interacting protein

## Introduction

Diabetes mellitus (DM) is associated with endothelial dysfunction including changes in barrier function and haemostasis, reduced vasodilator responses, inflammatory activation and increased angiogenesis, as well as more frequent and severe atherosclerotic cardiovascular diseases [1,2]. Hyperglycaemia is thought to affect endothelial function, increasing the stiffness of peripheral arteries and arterioles due, at least in part, to reduced nitric oxide production [1,2]. The increased formation of AGEs has been also acknowledged to play a relevant role in the development of vascular diabetic complications including atherosclerosis.